Influence of Electromagnetic Polarization on Whole-body Averaged SAR in Humans for Plane-wave Exposures

Akimasa Hirata, Naoki Ito, and Osamu Fujiwara
Department of Computer Science and Engineering, Nagoya Institute of Technology, Nagoya, Japan

E-mail: ahirata@nitech.ac.jp

Abstract

The present study investigated the whole-body averaged specific absorption rate (WBSAR) in an infant model with the finite-difference time-domain method. The focus of the present study is the effect of polarization of incident electromagnetic waves on the WBSAR. This is because most previous studies investigated the WBSAR for plane-wave exposure with a vertically aligned electric field. Our computational results revealed that the WBSAR for plane-wave exposure with a vertically aligned electric field is smaller than that with a horizontally aligned electric field for frequencies above 2 GHz. The main reason for this difference is attributed to be the component of the surface area perpendicular to the electric field of incident wave.

1. Introduction

There has been increasing public concern about adverse health effects of human exposure to electromagnetic (EM) waves. According to the International Commission on Non-Ionizing Radiation Protection (ICNIRP) safety guidelines [1998] and the IEEE standard [2006], whole-body averaged specific absorption rate (WBSAR) is currently used as a metric of basic restriction for radio frequency (RF) whole-body exposure. The limit of WBSAR is 0.4 W/kg for occupational exposure, or 0.08 W/kg for public exposure. An incident electric/magnetic field, which does not produce EM absorption exceeding the above basic limit, is used as a reference level in the ICNIRP guidelines [1998] and the maximum permissible exposure in the IEEE standard [2006]. The WBSAR depends largely on the frequency of the incident wave, despite of the same power density, and its peak appears at several dozen megahertz for adults [Gandhi, 1980]. Recently, the WBSAR in anatomically based human body models has been calculated in the RF frequency region under the ICNIRP reference level in accordance with the progress of computational resources [Conil et al. 2008, Dimbylow 2002, Dimbylow and Bolch 2007, Nagaoka et al. 2004, Hirata et al. 2007, Sandini 2003, Wang et al. 2007]. The WBSAR was found to have another peak around 2 GHz, which is caused by the relaxation of the reference level (e.g., Wang et al. 2007). The point to be stressed here is that the WBSAR of anatomically based human models around these peaks approaches the basic restriction provided in the

international standards/guidelines. Due to the spread of wireless communications, the WBSAR 2 GHz and above has received a great deal of attention. The above studies focused on the WBSAR for plane-wave exposure with vertically aligned electric field polarization (VP). The main reason for this would be that the WBSAR becomes maximal at several dozen megahertz for plane-wave exposure with VP at the same incident power density due to the standing wave over the body. In other words, whole-body exposure with VP was considered to be the *worst-case exposure*. However, Rowlandson and Barber [1979] reported the WBSAR for plane-wave with horizontally aligned electric field polarization (HP) to be larger than that for VP in the GHz region. Rowlandson and Barber used a theory of geometrical optics in their study. The allowable criterion of computational convergence was 10-20%. However, the effect of electromagnetic polarization on the WBSAR has not been revealed, although the difference in the reflection coefficient between VP and HP incident on the spheroid is a possible explanation. The main purpose of the present study is to investigate the influence of electromagnetic polarization on the WBSAR in the anatomically based human models in the GHz-frequency region.

2. Methods and Models

A. Computational Methods

The Finite-Difference Time-Domain (FDTD) method (Taflove and Hagness 2005) is used for

computational dosimetry. Either one of human models is located in free space. As a wave source, a plane wave with both vertical polarization (VP) and the horizontal polarization (HP) were considered. Plane wave is incident to the human from the front. The reason for choosing this scenario is that the WBSAR becomes maximal. Therefore, the WBSAR in this condition is essential from the aspect of the relationship between basic restriction and the reference level in the safety guidelines (ICNIRP, 1998).

A 24-layered uniaxial-Perfectly Matched Layer was used as the absorbing boundary. The separation between the model and the absorbing boundary was set at 100 cells. The electrical constants of tissues were taken from a report by Gabriel (1996). Validity and uncertainty of our computational codes have been confirmed via the intercomparison between three institutes (Dimbylow et al, 2008).

B. Computational Models

Whole-body voxel models for a Japanese adult male and a Japanese adult female were developed by Nagaoka et al. (2004). The resolution of these models was 2 mm segmented into 51 anatomical regions. Models for children of three, five and seven years of age were developed by applying a free form deformation algorithm to the male model. In this modeling, a total of 66 body dimensions was taken into account, and then reduced with different scaling factors

(Nagaoka et al 2008). Manual editing was applied in order to maintain their anatomical validity. The height and weight of seven-year-old, five-year-old, and three-year-old child models were 1.21 m and 23 kg, 1.04 m and 17 kg, and 0.88 m and 13 kg, respectively. The resolution of these models was kept to 2 mm. In the present study, these models were divided so that the resolution of the model becomes 1 mm, which is required for computational simulation with the FDTD method up to 6 GHz.

In the present study, a nine-month-old infant model was developed by linearly reducing a three-year-old Japanese infant model. The height and weight of the nine-month-old infant model are 0.70 m and 8.9 kg, respectively, with a resolution of 1 mm. The reason for developing the nine-month-old infant model is that the WBSAR in the nine-month-old infant is somewhat larger than that in three-year-old infant model (Dimbylow and Bolch 2007). The disadvantage of the newly developed infant model is that it was obtained by linearly reduced from the three-year-old infant model with a resolution 2 mm.

3. Computational Results

The nine-month-old infant model is used for fundamental discussion. The WBSAR in the nine-month-old infant model is plotted in Fig. 3 for VP and HP. For comparison, the WBSAR in the nine-month-old infant model developed at the University of Florida reported by Dimbylow

and Bolch (2007) is also plotted. As shown in this figure, the tendency of the present results and those of Dimbylow and Bolch (2007) are the same for exposure with VP, supporting the validity of our computational results. Comparing the WBSAR for exposures with VP and HP, the former is smaller than the latter for frequencies above 2 GHz.

In order to clarify the reason for this difference, in Fig. 2, we show the SAR distribution on the human body model for exposure with VP to that with HP, together with their ratio of voxel SAR. As shown in the figure, the SAR distribution is high at the front of the body. Some difference was observed around top and bottom and sides. From Fig. 2 (c), higher ratio is observed at the top of the head, the shoulders, the instep, and so on. In contrast, this ratio becomes smaller at the side of the body. Namely, higher SAR is observed at the body surface perpendicular to the electric field of the incident wave. At the front surface of the human body, the SAR with VP was comparable to that with HP (see Figs. 2 (a) and (b)).

In order to confirm the above finding, in Fig. 3, we show the SAR averaged over various body parts, i.e., the head and neck, the trunk, the arms, and the legs. The SAR averaged over the trunk is similar for the different polarizations. From the same figure, the average SAR for HP exposure is 2 - 8% larger than that for VP, mainly due to power absorption in the head and neck and/or the legs.

We show the relative difference of WBSAR between VP and HP for three-year-old,

five-year-old, seven-year-old child models in order to confirm if the above finding is valid for different models. From Fig. 4, the difference becomes large with the increase of the frequency. The difference for the seven-year-old models at 5 GHz was 15% or more.

4. Discussions and Conclusions

The present study investigated the WBSAR in the Japanese models with the FDTD method. We considered the influence of the polarization of the incident electromagnetic wave on the WBSAR. The computational results of the present study revealed that the WBSAR for a plane-wave exposure with VP was smaller than that with HP for frequencies between 2 and 6 GHz. As reported in Hirata et al. (2007), the dominant factor influencing the WBSAR in this frequency region is the surface area of the body model. This was confirmed from Fig. 2 (a) and (b), and 3; the power absorption at the front of the model is comparable to the cases for VP and HP. This figure confirms the finding of Hirata et al. (2007) that the dominant factor influencing the power absorption is the surface area of the body. Even for a body of the same surface area, however, a difference due to the different polarizations is observed, which is due mainly to the difference in the component of surface area perpendicular to the electric field of incident wave (see Fig. 3). A clear tendency was not observed for the arms. The reason for this discrepancy is the complicated structure of the arms and the surrounding structure, together with the diffraction

of electromagnetic waves. A large WBSAR for HP exposures compared to that for VP coincides with the results in 1970s. Note that a prolate spheroid was used as a human body model and computational convergence was at most 10-20%.

Future work is to investigate the tendency in frequencies above 6 GHz, since the computation cannot be conducted due to the limitation of computational resources.

Acknowledgement

The authors would like to thank Drs. Soichi Watanabe and Tomoaki Nagaoka for providing their anatomically based child model. This study was supported in part by KAKENHI through a Grant-in-Aid for Scientific Research (B).

REFERENCES

Conil E, Hadjem A, Lacroux F, Wong M F, and Wiart J 2008 Variability analysis of SAR from 20 MHz to 2.4 GHz for different adult and child models using finite-difference time-domain *Phys. Med. Biol.* **53** 1511-1525

Dimbylow P J 2002 Fine resolution calculations of SAR in the human body for frequencies up to 3 GHz *Phys. Med. Biol.* **47** 2835-2846

Dimbylow P and Bolch W 2007 Whole-body-averaged SAR from 50 MHz to 4 GHz in the University of Florida child voxel phantoms *Phys. Med. Biol* **52** 6639-6649

Dimbylow P, Hirata A, and Nagaoka T 2008 Intercomparison of whole-body averaged SAR in

European and Japanese voxel phantoms *Phys. Med. Biol.* **53** 5883-5897

Gabriel C 1996 Compilation of the dielectric properties of body tissues at RF and microwave frequencies, Final Tech Rep Occupational and Environmental Health Directorate. AL/OE-TR-1996-0037 (Brooks Air Force Base, TX: RFR Division

Hirata A, Kodera S, Wang J and Fujiwara O 2007 Dominant factors influencing whole-body average SAR due to far-field exposure in whole-body resonance frequency and GHz regions *Bioelectromagnetics* **28** 484-487

International Commission on Non-Ionizing Radiation Protection (ICNIRP) 1998 Guidelines for limiting exposure to time-varying electric, magnetic, and electromagnetic fields (up to 300 GHz)., *Health Phys.* **74** 494-522

Nagaoka T, Watanabe S, Sakurai K, Kunieda E, Watanabe S, Taki M, and Yamanaka Y 2004 Development of realistic high-resolution whole-body voxel models of Japanese adult males and females of average height and weight, and application of models to radio-frequency electromagnetic-field dosimetry *Phys. Med. Biol.* **49** 1-15

Nagaoka T, Kunieda E, and Watanabe S 2008 Proportion-corrected scaled voxel models for Japanese children and their application to the numerical dosimetry of specific absorption rate for frequencies from 30 MHz to 3 GHz *Phys Med Biol* (accepted)

Rowlandson G I and Barber P W 1979 Absorption of higher-frequency RF energy by biological models: Calculations based on geometrical optics," *Radio Sci.* **14** 43-50

Sandrini L, Vaccari A, Malacarne C, Cristoforetti L and Pontalti 2004 RF dosimetry:

comparison between power absorption of female and male numerical models from 0.1 to 4 GHz *Phys Med Biol* **49** 5185-5201

Taflove A and Hagness S 2003 Computational Electrodynamics: The Finite-Difference Time-Domain Method: 3rd Ed. Norwood. MA: Artech House

Wang J, Fujiwara O, Kodera S, Watanabe S 2006 FDTD calculation of whole-body average SAR in adult and infant models for frequencies from 30 MHz to 3 GHz *Phys. Med. Biol.* **51** 4119-4127.

FIGURE CAPTIONS

Figure 1. Frequency characteristics of whole-body averaged SAR from 1 to 6 GHz. The results reported by Dimbylow and Bolch (2007) are also plotted for comparison.

Figure 2. SAR distribution on the human body for plane-wave exposure with (a) vertical polarization and with (b) horizontal polarization. The distribution of the ratio of SAR between them is illustrated in (c).

Figure 3. Frequency dependency of SAR averaged over the head and neck, the trunk, the arms, and the legs.

Figure 4. Relative difference of whole-body averaged SAR between VP and HP for different human models.

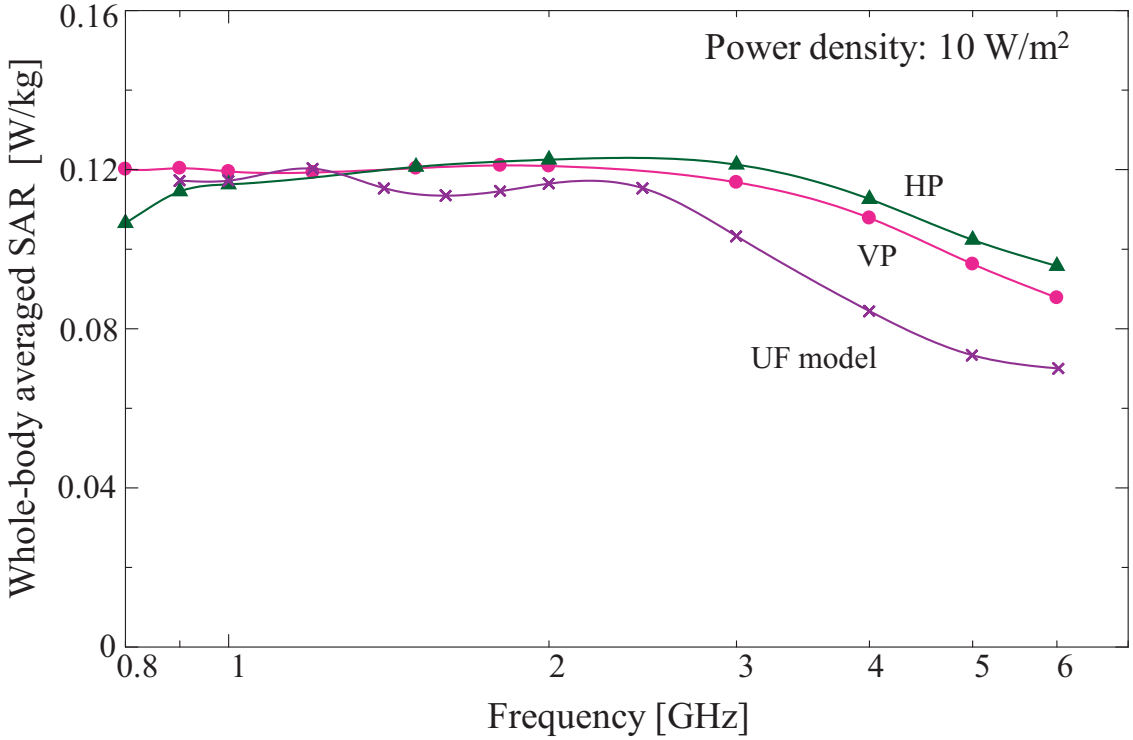
Power density: 10 W/m2
HP
VP
UF model
Whole-body averaged SAR [W/kg]
Frequency [GHz]
0.16
0.12
0.08
0.04
0
0.8
1
2
3
4
5
6

Figure 1

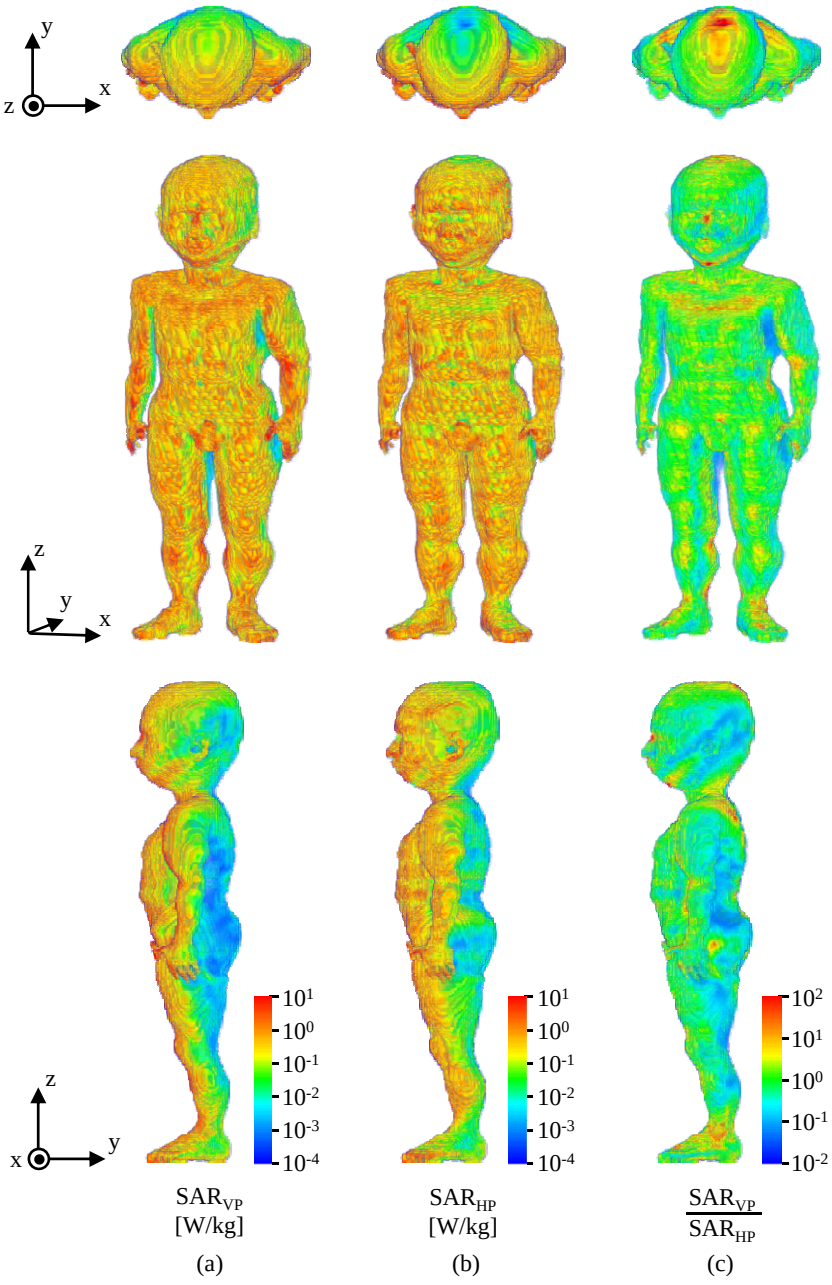

SAR_{VP} [W/kg] (a)

SAR_{HP} [W/kg] (b)

$\frac{SAR_{VP}}{SAR_{HP}}$ (c)

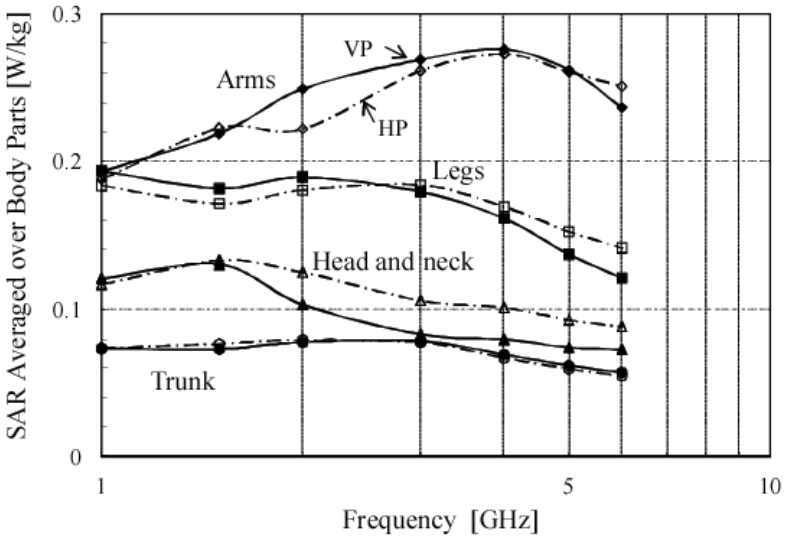
SAR Averaged over Body Parts [W/kg]
0.3
0.2
0.1
0
VP
Arms
HP
Legs
Head and neck
Trunk
1
5
10
Frequency [GHz]

Figure 3

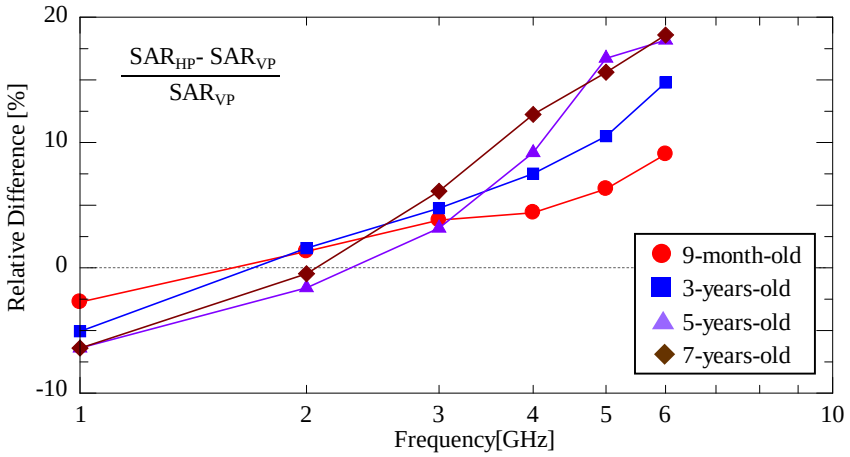
20
10
0
-10
1
2
3
4
5
6
10
Relative Difference [%]
Frequency[GHz]
SAR_HP- SAR_VP
SAR_VP
9-month-old
3-years-old
5-years-old
7-years-old

Figure 4